Suppression of Pulsed Interference through Blanking

Christopher Hegarty
Federal Aviation Administration, Washington, D.C.

A.J. Van Dierendonck
AJ Systems, Los Altos, CA

Dan Bobyn
Dan Bobyn Engineering Ltd., Calgary, Alberta, Canada

Michael Tran, Taehwan Kim
The MITRE Corporation, McLean, VA

Joe Grabowski
Zeta Associates, Fairfax, VA

BIOGRAPHIES

Dr. Christopher Hegarty received his B.S. and M.S. from Worcester Polytechnic Institute, and his D. Sc. from The George Washington University. He has been with The MITRE Corporation since 1992, most recently as a Project Team Manager. In August 1999, he began a one-year assignment as Civil GPS Modernization Project Lead with the FAA through the Intergovernmental Personnel Act. He was a recipient of the 1998 ION Early Achievement Award, and currently serves as Editor of *Navigation*: *Journal of the Institute of Navigation* and as co-chair of RTCA SC159 Working Group 1 (3rd Civil GPS Frequency).

Dr. A.J. Van Dierendonck received a BSEE from South Dakota State University and MSEE and Ph.D. from Iowa State University. Currently, he is self-employed under the name of AJ Systems and is a general partner of GPS Silicon Valley. In 1993, Dr. Van Dierendonck was awarded the Johannes Kepler Award by the Institute of Navigation Satellite Navigation Division for outstanding contributions to satellite navigation. For 1997, he was awarded the ION Thurlow award for outstanding contributions to the science of navigation. A.J. has 25 years of GPS experience and is a Fellow Member of the IEEE and ION. Recently, he was inducted into the GPS Joint Program Office's GPS Hall of Fame. He currently serves as working group co-chairman of the RTCA SC159 Working Group (WG1) for the 3rd Civil GPS Frequency.

Dan Bobyn is an RF engineer, who works full time as an RF and microwave circuit design consultant and contractor. He has spent the last 21 years working with and for companies designing navigation and communications equipment. He holds a B.Sc. in EE from the University of Saskatchewan.

Dr. Michael Tran received his BSEE, MSEE, and Ph.D. from Virginia Tech. Prior to joining The MITRE Corporation in September 1999, he worked at Texas Instruments for 2 years and at Stanford Telecom for 4 years in the area of satellite communications, DSP algorithm coding, and receiver VHDL algorithm coding.

Taehwan Kim is a lead engineer in MITRE CAASD. Before joining CAASD in 1997, he worked for STel and Hughes for 10 years supporting NASA satellite communications. He received his B.S. in mathematics from Seoul National University, M.S. in Computer Science from the University of South Carolina, and is pursuing a Ph.D. in EE at the University of Maryland.

Joe Grabowski received his B.S.EE from Carnegie-Mellon University and M.S.EE from Purdue University. Since 1990 he has been working at Zeta Associates on various communications and digital signal processing projects as a systems engineer. Previously he has worked at ESL Inc. from 1984 to 1990 also as a systems engineer and at Harris Corporation from 1978 to 1982 as an analog circuit designer.

ABSTRACT

In November 1999, the Interagency GPS Executive Board (IGEB) endorsed a set of recommendations on implementing the third civil GPS frequency (L5) that included certain measures to be taken within the United States to ensure that L5 can coexist with government systems operating at the same or nearby frequencies.

These recommendations were based on analyses conducted in 1999 that assumed that pulse blanking is employed by GPS L5 user equipment. This paper describes the impact of pulsed interference on GPS user equipment and presents the results of simulation and hardware tests that were conducted this year to validate the assumed performance of L5 user equipment with blanking.

INTRODUCTION

In November 1999, the Interagency GPS Executive Board (IGEB) endorsed a set of recommendations on implementing the third civil GPS frequency (L5) [1] that included certain measures to be taken within the United States to ensure that L5 can coexist with government systems operating at the same or nearby frequencies. Specifically, the IGEB recommendations included that:

1. The new L5 signal structure proposed in [2] be implemented.
2. The L5 signal be implemented with minimum received signal power at –154 dBW (6 dB higher than the L1 C/A code).
3. If the Department of Defense (DoD)'s proposal for updated spectrum certification of Link 16 is approved through the established National Telecommunications and Information Administration (NTIA)/ Interdepartment Radio Advisory Committee (IRAC) process, the DoD will increase the operational management of Link 16 Time Slot Duty Factor (TSDF).
4. In the United States, the Federal Aviation Administration (FAA) will regionally reassign Distance Measuring Equipment (DME)/Tactical Air Navigation (TACAN) within +/-9 MHz of 1176.45 MHz as necessary.
5. The DoD will include a priced option in the full-rate production Multifunctional Information Distribution System (MIDS) frequencies in the 960 – 1215 MHz band.

Importantly, these recommendations were based entirely on analytical analyses conducted in 1999. In order to validate some of the critical underlying assumptions, an ad hoc Working Group (WG1, Validation of Coexistence) of the IGEB was established earlier this year. This paper describes software simulations and hardware tests that were performed under the auspices of WG1 to validate the performance of L5 user equipment using blanking to suppress pulsed interference. The paper first provides some background information on the effects of pulsed interference on GPS receivers without blanking, and an overview of pulse blanking.

EFFECTS OF PULSED INTERFERENCE ON GPS RECEIVERS

The effects of pulsed interference on GPS receivers can vary widely depending on the characteristics of the received interfering signal (peak power, duty cycle, pulse width) and the exact implementation of the receiver. Very strong pulsed signals can cause problems even during their "off" state, since active components in the GPS receiver may require "recovery" time after a pulse to resume normal operation. As illustrated in Figure 1, all electronic amplifiers saturate when the input signal reaches some level (i.e., amplifiers cannot continue to provide constant gain with only finite power available). Typical amplifier output levels at the point of saturation range from 0 to 20 dBm for commercial GPS receivers (usually towards the higher end of the range for later gain stages in the front-end).

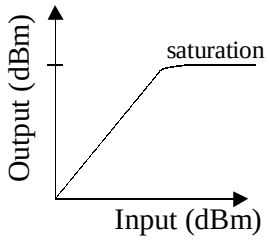

Figure 1. Amplifier Saturation

Of greater interest is the power level needed at the antenna output port to saturate the receiver. Determination of this level, as a function of frequency, requires careful analysis of the entire receiver front-end. In-band pulses will typically saturate the last gain stage first. For one commercial receiver design that was looked at in detail, this last gain stage is designed to provide 15 dB of headroom above the normal thermal noise level at that stage. For this design, an in-band pulsed signal with peak power of –85 dBm at the antenna output port will saturate the front-end. Interference sources at frequencies offset from the center of the receiver passband require progressively larger amplitudes to saturate the receiver front-end as that frequency offset increases. Near-band interference will tend to saturate the intermediate gain stages with medium-level input interference, and out-of-band interference signals will saturate only the first radio frequency (RF) stages of the front-end. This characteristic is due to the interspersing of filters between each RF and Intermediate Frequency (IF) gain stage, which leads to increasing frequency selectivity as the interference signal proceeds through the front-end.

Near-band and out-of-band pulses can saturate radio frequency (RF) gain stages first, since these stages precede highly selective intermediate frequency (IF) filters that protect later IF gain stages.

Figure 2, created through SPICE (Simulation Program with Integrated Circuit Emphasis) simulations, shows recovery times required by discrete and monolithic microwave integrated circuit (MMIC) amplifiers typical of those used in commercial GPS receivers. The results indicate that recovery times of approximately 40 ns/dB of input level beyond the saturation point is typical for active stages in commercial GPS receivers. It should be noted, however, that today's commercial receivers are not built to operate in a pulsed environment. Prudent design measures for L5 would include raising the saturation levels for some active stages, and designing these stages to recover more rapidly in the event of a saturating pulse. With careful design, it is anticipated that recovery times of a few hundred nanoseconds can be practically implemented.

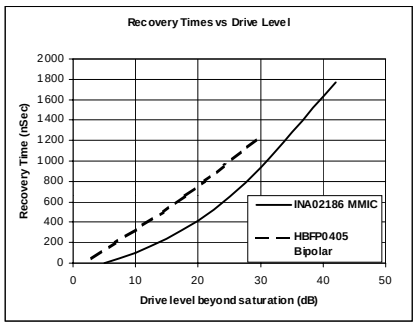

Figure 2. Recovery Times for Typical Discrete and MMIC Amplifiers

Strong pulses will also saturate the analog-to-digital (A/D) converter in GPS receivers. A/D saturation is actually a beneficial event in that it limits the amount of pulse energy that enters the correlators. When the A/D is being saturated by a pulse, the desired signal is completely suppressed.

Weaker pulses (those that do not saturate active stages or the A/D) may be viewed as adding to the receiver's noise floor. As will be discussed in more detail later, the degradations to receiver functions depend on the power spectral density of the pulsed signal. Data demodulation is very sensitive to pulse width as well. This paper focuses exclusively on short-pulsed interference, expected at or near L5, which is characterized by many pulses within each data symbol.

Automatic Gain Control (AGC) effects are also very important with pulsed interference. An AGC is needed with multibit A/Ds to properly set the A/D input level to minimize signal-to-noise losses due to quantization. As shown in Figure 3 [3], A/D quantization losses for common 2-bit and 3-bit implementations can increase significantly if the signal level at the A/D input is not properly maintained.

The presence of pulsed interference will degrade the performance of slow AGCs (typical in commercial receivers) unless preventative measures are taken. Slow AGCs set the A/D input levels based on average signal power averaged over pulse "on" and pulse "off" conditions and thus the quantizer levels are not properly set for either condition. Consider the effect of strong pulsed interference. The slow AGC will correctly determine the increase in the root mean square (rms) signal voltage. The AGC will then decrease the signal level entering the A/D (or equivalently increase the quantizer input levels), which increases quantization losses for those periods of time between pulses (the only periods of time when the desired signal is not suppressed). With weak interference present a similar degradation occurs when the pulses are not present. In addition, when the pulses are present, the AGC sets the A/D input level too high. A fast AGC would solve these problems. Increasing the number of A/D bits would alleviate the problems, since performance is no longer as sensitive to threshold settings (see Figure 3). However, adding bits decreases benefits from quantizer limiting of pulse energy.

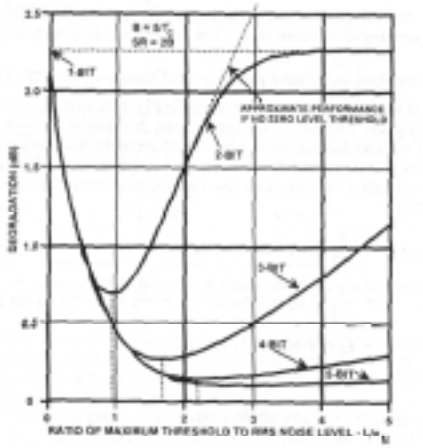

Figure 3. Quantization Implementation Losses as a Function of AGC Input Signal Level Setting [3]

PULSE BLANKING

Pulse blanking is a simple technique to suppress pulsed interference by having the A/D output zeroes when a pulse is detected. Pulse detection, for strong pulses, is not difficult since the received GPS signals are buried beneath thermal noise. Pulse detection may be accomplished using analog power measurements or, nearly-equivalently, implemented digitally by analyzing histograms of the A/D output levels in real-time. With either method, careful AGC implementation is necessary to minimize quantization losses. For instance, when using the histogram method, quantizer output samples that have been determined to correspond to the reception of strong

pulses should be discarded from use in determining A/D input levels since these samples would result in improper quantizer level thresholds. Careful design is also required to ensure that the receiver will blank any input signals that are strong enough to saturate the front-end.

It should be noted that blanking is not the optimal technique for pulse suppression. Given a general received signal of the form:

$$r(t) = s(t) + I(t) + n(t) \quad (1)$$

where s(t) is the desired signal, I(t) is interference (pulsed or continuous), and n(t) is additive white gaussian noise, it is straightforward to show that if I(t) is perfectly known, optimal estimation of certain parameters of the desired signal (e.g., time of arrival) involves interference excision (i.e., computation of r(t) – I(t)). If some parameters of I(t) are unknown (e.g., time-of-arrival, amplitude), but can be well-estimated as in the case of a very strong pulsed signal, optimal estimation of some parameters of the desired signal again involves interference excision. This approach was not pursued as a minimum requirement for L5 user equipment, since it requires a very linear front-end (i.e., many A/D output bits), which was not deemed practical. In contrast, blanking is very simple to implement and does not even require a multi-bit receiver. It can be viewed as near-optimal in the sense that it completely excises strong pulsed interference, at the expense of complete suppression of the desired signal during the strong pulses.

PERFORMANCE OF PULSE BLANKING

With one strong-pulsed signal present, perfect blanking results in a signal-to-noise ratio (SNR) degradation of $10\log(1\text{-}PDC_B)$ where PDC_B is the duty cycle of the blanking signal. This SNR degradation follows from the fact that when the strong pulses are present, blanking completely suppresses the desired signal (a $20\log(1\text{-}PDC_B)$ SNR degradation), but also completely suppresses the thermal noise (a $10\log(1\text{-}PDC_B)$ SNR gain).

A more detailed equation [4] that was used for computing the S/N_0 degradation to an L5 receiver in the analyses that led to the IGEB recommendations in November 1999 is:

$$S/N_{0,\text{eff}} = 39.5 + 20\log(1 - PDC_B) - 10\log\left(1 - PDC_B + \sum_{i=1}^{N} 10^{\left(\frac{R_i}{10}\right)}\right) \quad (2)$$

where

$$(R_i)_{dB} = P_i + 97\ \text{dBm} + 10\log dc_i, \quad (3)$$

PDC_B (pulse duty cycle – blanker) is the total duty cycle of all pulses strong enough to activate the blanker, N is the total number of low-level undesired received signals (i.e., those not strong enough to trip the blanker), P_i is the peak received power of the i-th undesired signal, and dc_i is the duty cycle of the i-th low-level signal. Importantly, this equation is only valid when the pulses are very short relative to the minimum predetection integration time used by the receiver (1 – 10 ms, depending on the mode of operation). This constraint is satisfied for the sources of emission of concern near L5.

The formulation of this equation included several simplifying assumptions. First, the equation conservatively assumes that pulses never collide, thus strong pulses never suppress weak ones, and duty cycles are directly summed. Second, a highly simplified correlation model is used that assumes that weak pulse energy is spread evenly across the 20 MHz L5 signal null-to-null bandwidth by correlation of the interference with the replica L5 codes. More refined correlation models are described later in this paper.

Because analyses based on this equation (with an assumed 1 μs pulse detection delay) directly led to the recommendations in [1], IGEB WG1 efforts have focused on validating its accuracy. The next two sections present software simulation and hardware tests that were performed for this purpose.

SOFTWARE SIMULATIONS

As one means to verify L5 receiver performance in the presence of pulsed interference, a high fidelity software simulation of a GPS/Wide Area Augmentation System (WAAS) single-channel receiver was developed. The simulation emulated a GPS/WAAS L5 receiver beginning with modeled analog inphase (I) and quadraphase (Q) IF received signals sampled at 40 Msamples/s. A 20 MHz two-sided receiver front-end bandwidth was emulated using a four-pole low-pass filter. The I and Q samples were then quantized into 3 bits (8 levels), and correlated with early, late, and prompt samples of replica L5 I (I5) and Q (Q5) codes (including the L5 Neuman-Hoffman codes [5]). The correlator outputs, integrated over 10 ms for GPS, or 2 ms for WAAS, were subsequently processed to form carrier phase, code phase, and bit estimates.

A third-order carrier phase loop was implemented using the loop filter formulation from [6]. A phase locked loop (PLL) with a 10 Hz loop bandwidth was implemented using the Q5 channel for GPS. A Costas loop with a 10 Hz loop bandwidth was implemented for WAAS signal phase tracking (note that the WAAS L5 signal was

assumed to only include an I5 code with no quadrature channel).

The code phase tracking loop used a first-order early-minus-late power delay locked loop (DLL) with carrier aiding (operating on the Q5 channel for GPS). Early-late spacing was set at 0.5115 L5 chips (2 samples at the 40 MHz sampling rate). The code tracking loop bandwidth was set at 5 Hz. This unusually large code loop bandwidth was selected to allow collection of closed loop error statistics with reasonable run times (on a 450 MHz computer, one simulated receiver second took about 3 min to run). A limited number of extremely long runs were conducted using a 0.05 Hz loop bandwidth to verify the expected linear proportionality between loop bandwidth and tracking error variance.

Data demodulation was accomplished with 3-bit soft-decision Viterbi decoding of the 50 bps GPS data (250 bps WAAS data).

Analog pulse detection was emulated by adding the squares of the IF I and Q samples to form an instantaneous power estimate, and then smoothing this estimate using a first-order digital filter with a 0.25 μs time constant. The smoothed power estimate was compared with a threshold consistent with a peak received power level of –86.5 dBm at the antenna output port. This level is more than 10 dB above the ambient noise power level of –97 dBm. The threshold level was selected to be high enough to preclude undesired blanking in the event of a continuous interference source [4].

Calibration

To ensure the simulation was working properly, its outputs were carefully calibrated against theory prior to adding any pulsed interference. The predicted variance (in radians squared) for a PLL tracking the Q5 code in a GPS L5 receiver is [7]:

$$\sigma_\phi{}^2 = \frac{2B_\phi}{S/N_0} \tag{4}$$

where B_ϕ is the loop bandwidth.

The predicted code tracking variance (in code chips squared) for a DLL tracking the Q5 code is:

$$\sigma_\tau{}^2 = \frac{2B_L(1-0.5B_L T)\int_{-\infty}^{\infty} S_c(f)\left|H(f)\right|^2 \sin^2(\pi f d T_c)\,df}{(2\pi)^2 S/N_0 \left(T_c \int_{-\infty}^{\infty} f S_c(f)\left|H(f)\right|^2 \sin(\pi f d T_c)\,df\right)^2} \tag{5}$$

where B_L is the code tracking loop bandwidth, H(f) is the frequency response of the bandlimited front-end, $S_c(f)$ is the power spectral density of the spreading code, d is the chip spacing (in L5 code chips), and T is the predetection integration time.

Equation (5) is based on [8] with modifications to account for the power split between the I5 and Q5 channels, and also to account for the implemented bandlimiting of the front-end (perfect filtering is assumed in [8]).

Figure 4 plots the standard deviation of the code and carrier phase tracking errors (as circles) for the simulated GPS L5 receiver based on simulated receiver operating period of 33 s. Also shown on the figure (as solid lines) are the theoretical results, calculated from equations (4) and (5) after applying input SNR corrections to account for quantization losses (0.4 dB) and signal losses due to the bandlimiting (0.5 dB). The 0.5 dB signal loss correction was only applied to carrier tracking, since equation (5) implicitly accounts for this effect.

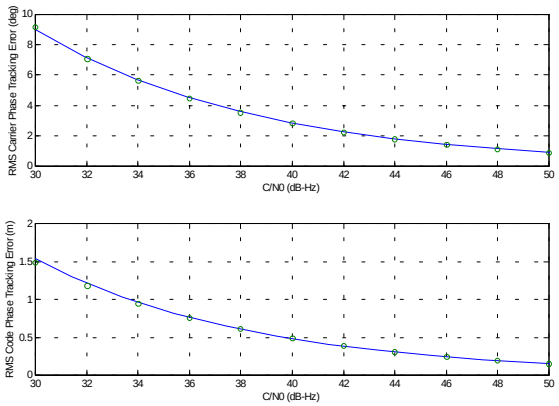

Figure 4. Simulation Calibration Results - GPS

Strong Pulse Results

To validate equation (2) in the presence of strong pulses, the simulation input signal was corrupted by pulsed interference with peak power level of –74 dBm (above the blanker threshold). The pulse repetition interval was held fixed at 12 μs and the duty cycle was increased from 0 to 90 percent (see Figure 5) to produce pulsewidths consistent with those expected near L5 [4]. The input SNR, without interference, was set to 41.5 dB-Hz [4].

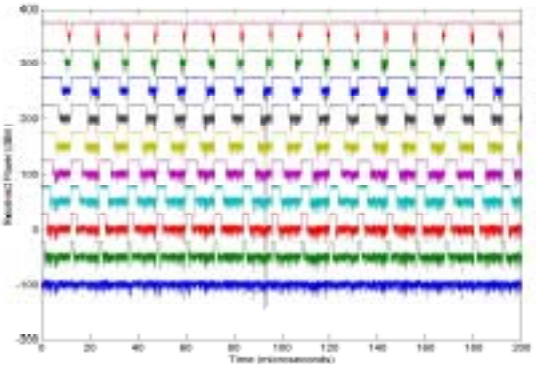

Figure 5. Square Pulse Inputs (vertical bias added to facilitate viewing)

The standard deviation of the simulated carrier phase and code tracking errors are shown in Figure 6 (as circles) as a function of duty cycle. Also shown on the figure (as solid lines) are the predicted errors, based on (4) and (5) with input SNR adjusted by the implementation loss corrections (described above) and $10\log(1\text{-}PDC_B)$ (which is what the SNR reduction predicted by equation (2) reduces to when only strong pulses are present). Note the excellent agreement. No data bit errors occurred over any of the 33 s runs.

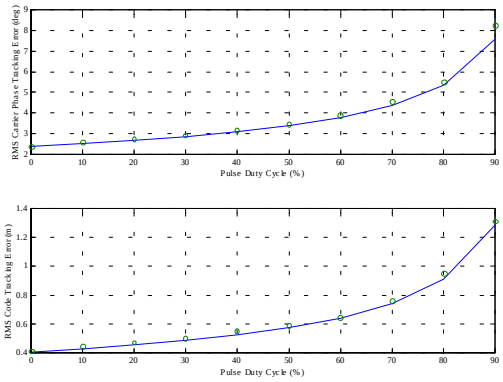

Figure 6. Strong Square Pulse Simulation Results - GPS

Weak Pulse Results

To validate equation (2) in the presence of weak pulses, the simulation input signal was corrupted by pulsed interference with peak power level of –88 dBm (below the blanker threshold). The pulse repetition interval was again held fixed at 12 μs and the duty cycle was increased from 0 to 90 percent. The input SNR, without interference, was set to 41.5 dB-Hz [4].

No data bit errors were observed. The standard deviation of the simulated carrier phase and code tracking errors are shown in Figure 7 (as circles) as a function of duty cycle. Also shown on the figure (as solid lines) are the predicted errors, based on (4) and (5) with input SNR adjusted by $-10\log(1+10^{(Pi+97)/10}dc_i)$ (as predicted by equation (2)). In this case, equation (2) predicted much greater degradations to carrier phase and code tracking than were observed. It was speculated that this discrepancy was mostly due to the correlation model used. As stated earlier, equation (2) assumes that correlation with the reference spreading waveform spreads the interference signal uniformly over the reference waveform's two-sided bandwidth.

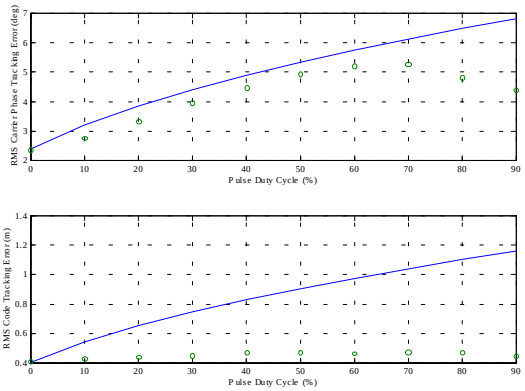

Figure 7. Weak Square Pulse Simulation Results - GPS

Two improved correlation models are shown in Figure 8. The model illustrated in Figure 8a is well-known and an equation for the effective interference power spectral density (psd) derived from this model [3]:

$$I_{0,eff} = \int_{-\infty}^{\infty} S_C(f) S_I(f) df \,, \qquad (6)$$

where $S_C(f)$ is the normalized psd of the reference spreading waveform and $S_I(f)$ is the psd of the interfering signal, accurately predicts degradations to carrier tracking, data demodulation, and acquisition from the presence of non-white interference.

The second correlation model, shown in Figure 8b is not so well-known. The model in Figure 8a is often misapplied to predict code tracking degradations due to interference. Proper analysis of interference effects on code tracking must take into account the correlation between early- and late-correlator outputs [8,9]. An equation for the effective interference psd for Figure 8b is:

$$I_{0,eff} = \frac{2}{d} \int_{-\infty}^{\infty} S_C(f) \sin^2(\pi f d T_c) S_I(f) df \,, \qquad (7)$$

where d is the spacing between the early and late correlator outputs (in code chips) and T_c is the code chip period.

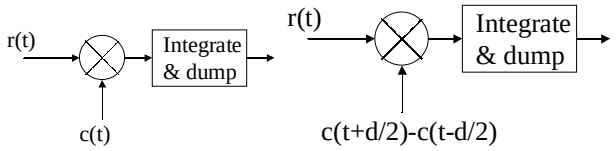

(a) (b)

Figure 8. Weak Pulse Correlation Models for (a) Carrier Tracking, Data Demodulation, and Acquisition, and (b) Code Tracking

To evaluate these improved correlation models, quantization was disabled in the simulations (to isolate correlation effects from A/D effects) and the code and carrier phase error statistics from simulation was compared to equations (4) and (5) with the input SNR in those equations replaced with:

$$\frac{S}{N_{0,\text{eff}}} = \frac{S}{N_0 + I_{0,\text{eff}}} \tag{8}$$

The comparison yielded very close agreement between simulation and theory (see Figure 9, simulation results are shown as circles, theory as solid lines). Note that the lack of degradation in the code tracking performance as the duty cycle of the pulsed signal was increased is due to the fact that the simulated early-late DLL with d = 0.5115 chips is insensitive to interference with power concentrated tightly about the carrier frequency (as predicted by equation (7)). The simulated interference waveforms fall into this category.

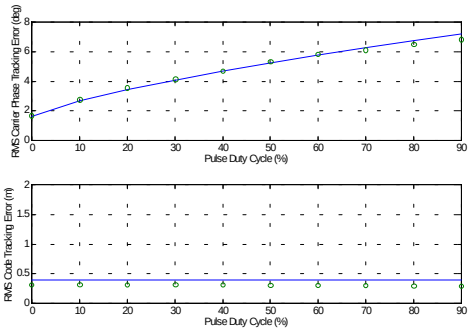

Figure 9. Comparison of Weak Square Pulse Simulation Results (with A/D Removed) to Improved Theory

Emulated L5 Environment Results

To evaluate the spectral environment near L5, a measurement campaign was conducted by participants in IGEB WG1. Signature waveforms, in the time domain, of emitters that operate at or near L5 have been digitized and recorded. Data (100 Msample/s, 10 bits/sample) has thus far been collected from DMEs, Joint Tactical Information Distribution System (JTIDS), and various radars (AN/TPS-59, AN/TPS-124, Millstone Hill) using a data collection system with a passband of 30 MHz centered at L5.

To date, a limited number of simulations have been conducted using the recorded signature waveforms as building blocks to reconstruct the current spectral environment for L5. As one example, Figure 10 plots the emulated time-domain signal that would be seen by an L5 receiver (DME/TACANs only) at 40,000 ft above Harrisburg, Pennsylvania, an area in the United States with a particularly challenging environment for L5 [4]. This signal was provided as the input to the L5 receiver simulation. The input SNR, before the interference was included, was set to 41.5 dB-Hz. The results with the interference included was a degradation in receiver SNR varying from 3 to 7 dB (as estimated from the code and carrier phase tracking statistics) over time. The time variation in SNR was due to random arrival times of the pulses received from the dozens of visible DME/TACANs, which produced a variation in duty cycle of the aggregate signal seen by the receiver. For comparison, equation (2) as it was applied for IGEB deliberations predicted a 13 dB SNR degradation. The reason for the discrepancy is that in the IGEB deliberations, pulses were conservatively assumed to never collide. This assumption was made largely to avoid the difficult question of how much credit to take for overlapping pulses. The question could be avoided within the United States, since reassigning the frequencies of DMEs near L5 is not difficult to plan for, given current U.S. plans to decommission a large number of these systems in the future. Other nations that would like to use L5 at high altitudes while retaining a large number of DMEs may wish to entertain this question.

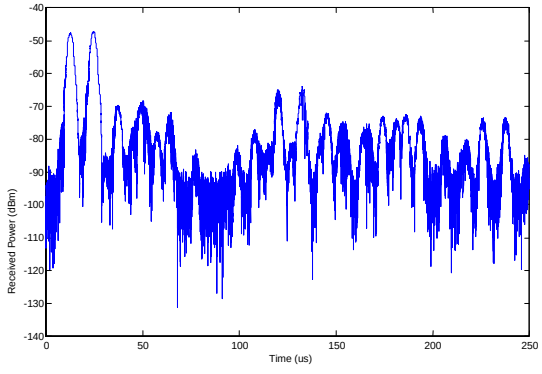

Figure 10. Emulated DME/TACAN Environment at 40,000 ft Above Harrisburg, Pennsylvania

HARDWARE TESTS

As a second validation activity, a hardware prototype blanking receiver was built [10]. The prototype (see Figure 11) was designed to receive standard L1 GPS signals in the presence of an externally generated test interference signal. The platform uses a custom RF front-end, a modified off-the-shelf GPS receiver and an external power supply module.

To facilitate system level testing, the custom RF front end incorporates:

- A GPS L1 Low Noise Amplifier (LNA), as normally found in an external active antenna,
- The losses of the antenna to receiver interconnecting cable, and,
- The receiver functions of RF signal down-conversion, AGC and amplification.

Relative to standard L1 receiver circuits, this front-end (see Figure 12) provides enhanced RF filter selectivity and incorporates pulse interference blanking circuits.

A modified NovAtel MiLLennium® OEM3 series receiver tracks the received L1 signals after they are down-converted in the custom RF front end. The signal interface between the OEM3 and the custom RF front end is at IF.

A special software load is contained in the OEM3 receiver. This software allows the receiver to perform P code signal handoff and straight P code tracking. Thus, the effect of pulsed interference can be evaluated for wide-band pseudonoise (PN) codes, similar to L5.

Figure 11. Hardware Prototype Blanking Receiver

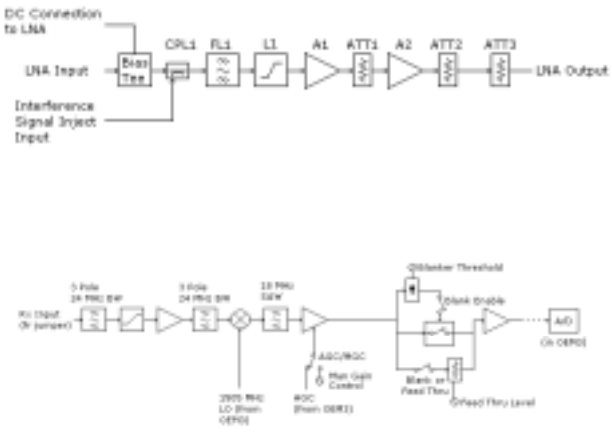

Figure 12. Functional Overview of Prototype Receiver

Strong Pulse Tests

To test equation (2) in the presence of strong pulses, the hardware prototype's input signal (from a GPS satellite signal generator) was corrupted using a Rohde & Schwarz SMT-03 synthesizer with a pulse modulation capability. Data was logged from the NovAtel OEM-3 receiver board related to carrier to noise level, lock status and the AGC level the receiver operated at. The typical test scenario would collect data without any interference for a period from 3 to 5 min followed by some kind of pulsed interference over the same time period. The interval without interference established a baseline for assessing loss in carrier to noise and also confirmed that the receiver was operating properly. Pulse widths were varied from 100 μs to as little as 1 μs while duty cycles were varied from 2.5 percent to 80 percent and pulsed interference power levels were varied from as little as –100 dBm to as high as –50 dBm.

Initial test results (see Figure 13) showed significant discrepancy between the theory of equation (2) and the prototype measurements. The discrepancy increased as the pulse widths were decreased. Close examination of the input signals to the A/D (see Figure 14) revealed that the analog blanker exhibited turn-on and turn-off lags, and also that the switching in and out of the attenuators that blanked the A/D input signal resulted in undesired signal transients. Figure 14(a) shows the A/D input signal with blanking disabled. A pulse is clearly present over the time interval from 0 to 5 μs. An ideal blanker would zero the input signal over that time period. The prototype blanker produced the A/D input signal shown in Figure 14(b). A turn-on delay of around 1.5 μs is evident, followed by another 0.5 μs of ringing by the attenuator being switched in. At 5 μs, when the pulsewidth ends, a 1.5 μs blanking turn-off delay can be seen, followed by another 0.5 μs of attenuator ringing as the attenuator is switched out. These

reaction lags and ringing clearly significantly reduced the effectiveness of blanking in this particular analog realization.

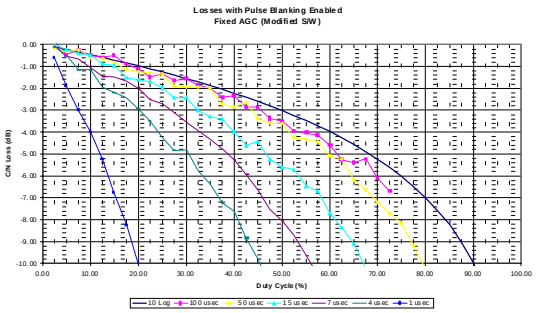

Figure 13. Initial Strong Pulse Hardware Test Results

To evaluate equation (2) with a nearly perfect blanker, a second strong pulse test was performed. In this test, the blanking circuitry of the prototype receiver was disabled. A mixer was inserted between the IF output of the prototype front-end and the A/D input on the NovAtel receiver. The SMT-03 pulse generator was used, with some auxiliary circuitry, to use the mixer as a fast analog switch that turned off during the synthesized pulses. The A/D input signal and pulsed switch-control waveform are shown in Figure 15. Note that the blanking of the input signal appears nearly instantaneous on the time scale of the plot. The recorded SNR degradations during this induced blanking test very closely matched equation (2) (see Figure 16), indicating that a fast-reacting analog blanking mechanism could in fact be as effective as predicted by theory.

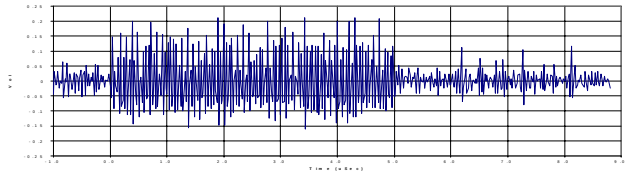

(a)

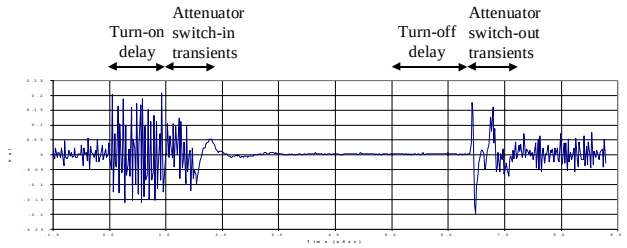

(b)

Figure 14. IF Output (a) without and (b) with Blanking Enabled

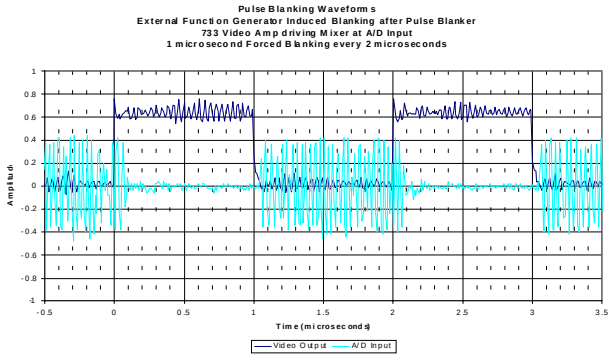

Figure 15. A/D Input with Induced Blanking

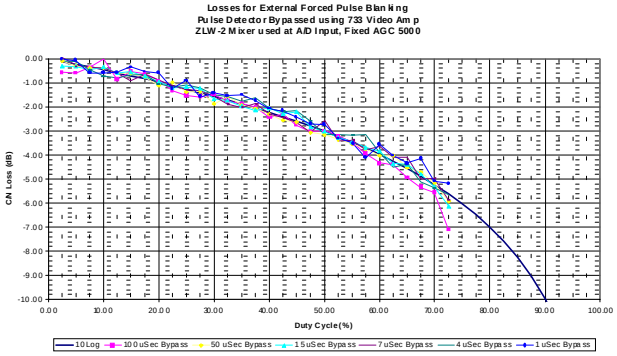

Figure 16. Strong Pulse Hardware Test Results with Induced Blanking

Weak Pulse Tests

To test equation (2) in the presence of weak pulses, the hardware prototype's blanking circuitry was disabled and the input was again was corrupted using the SMT-03 pulse generator. The results for pulsed interference with varied peak power and duty cycle are shown in Figure 17. Nearly identical curves resulted over a range of pulse widths from 1 to 100 μs. Also shown in Figure 17 are the predicted degradation curves based on equation (2) with one slight adjustment (the noise floor of the prototype equipment was lower than the –97 dBm level assumed in equation (3)). In general, the agreement was very good. The discrepancies, especially for the –85 dBm peak power case, can be explained by the fact that the prototype equipment operates with a slow AGC, and quantizes the signal with 6 digital output levels (see earlier discussion).

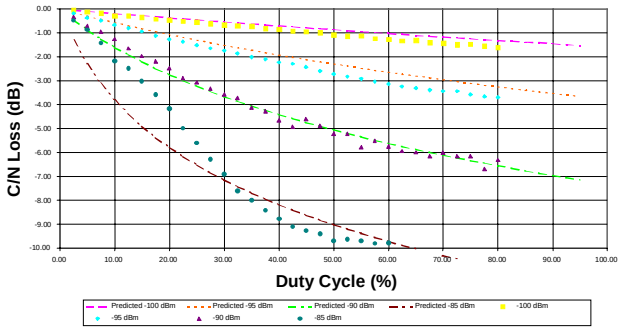

Figure 17. Weak Pulse Hardware Test Results

SUMMARY AND CONCLUSIONS

Blanking has been shown, through high-fidelity simulation and hardware testing, to be an effective means to combat pulsed interference. A simple equation that was used by the IGEB for long-range spectrum planning has been shown to very accurately predict the performance of blanking for strong pulses. The equation is not nearly so accurate for weak pulses, but is adequate for its intended purpose of providing a computationally simple means of evaluating the spectral environment for L5 for the purpose of long-range systems planning. Improved correlation models were described that more accurately predict weak pulse effects. However, these models require additional input information on both the interfering signal (power spectrum) and L5 receiver (early-late correlator spacing).

Application of the simple equation with the assumption that pulses do not collide has been shown to be very conservative. This conservatism has been acceptable within the United States, since a resulting decision to reassign the frequencies of DMEs near L5 is not difficult to plan for. Other nations that would like to use L5 at high altitudes while retaining a large number of DMEs may wish to revisit this assumption.

ACKNOWLEDGMENTS

The authors would like to thank the participants of IGEB Working Group 1 for their contributions to the simulations and hardware tests.

REFERENCES

[1] Anon., *Implementation of a Third Civil GPS Signal: Final Report, Interagency GPS Executive Board, November 2, 1999.*

[2] Van Dierendonck, A.J., and J.J.Spilker, “Proposed Third Civil GPS Signal at 1176.45 MHz: In-Phase/Quadrature Codes at 10.23 MHz Chip Rate,” *Proceedings of The Institute of Navigation Annual Meeting*, Cambridge, Massachusetts, June 1999.

[3] Van Dierendonck, A. J., “GPS Receivers,” *Global Positioning System: Theory and Applications*, B. Parkinson and J. J. Spilker, Jr., Ed., Washington, D.C.: AIAA, Inc., 1996.

[4] Hegarty, C., T. Kim, S. Ericson, P. Reddan, T. Morrissey, and A.J. Van Dierendonck, “Methodology for Determining Compatibility of GPS L5 with Existing Systems and Preliminary Results,” *Proceedings of The Institute of Navigation Annual Meeting*, Cambridge, MA, June 1999.

[5] Anon., *NAVSTAR GPS L5 Civil Signal Specification*, Draft 8, RTCA, Inc., Washington, D.C., June 13, 2000.

[6] Stephens, S.A., and J.C. Thomas, "Controlled-Root Formulation for Digital Phase-Locked Loops," *IEEE Transactions on Aerospace and Electronic Systems*, January 1995.

[7] Hegarty, C., *Evaluation of the Proposed Signal Structure for the New Civil GPS Signal at 1176.45 MHz*, The MITRE Corporation, Working Note WN99W34, McLean, Virginia, June 1999.

[8] Kolodziejski, K., and J. Betz, Effect of Non-White Gaussian Interference on GPS Code Tracking Accuracy, The MITRE Corporation, MITRE Technical Report MTR99B21R1, Bedford, Massachusetts, June 1999.

[9] Lopez-Almansa, J.-M., and P. Pablos, “Derivation of an Analytical Model for Estimation of Measurement Errors Induced by an Arbitrary Disturbance on a Coherent Delay Locked Loop,” *Proceedings of The Institute of Navigation Annual Meeting*, June 1998.

[10] Bobyn, D., *AJ Systems L5 Receiver Prototype (Hardware Part No. 9911002) Documentation Package*, Revision 0, Dan Bobyn Engineering Ltd., Calgary, Alberta, Canada, October 18, 1999.